A&A 426, 721–728 (2004)
DOI: 10.1051/0004-6361:20041088

Astronomy & Astrophysics

Tests with a Carlina-type hypertelescope prototype

I. Demonstration of star tracking and fringe acquisition with a balloon-suspended focal camera

H. Le Coroller[1], J. Dejonghe[1], C. Arpesella[1], D. Vernet[2], and A. Labeyrie[1]

[1] Laboratoire d'Interférométrie Stellaire et Exo-planétaire & Collège de France, Observatoire de Haute-Provence, 04870 St-Michel l'Observatoire, France
e-mail: coroller@obs-hp.fr
[2] Collège de France, Observatoire de la Côte d'Azur, Avenue Nicolas Copernic, 06130 Grasse, France

Received 15 April 2004 / Accepted 28 June 2004

Abstract. Labeyrie (1996, A&A, 118, 517) established the feasibility of snapshot images with a multi-aperture interferometer having a densified exit pupil. The numerous widely spaced mirrors in these instruments, called hypertelescopes, do not alleviate the usual difficulty of adjusting and phasing interferometers. A simplification is however possible, in the form of the optical and mechanical architecture called Carlina (Labeyrie et al. 2002, Proc. SPIE, 4838). It is configured like a diluted version of the Arecibo radio-telescope. Above the diluted primary mirror, made of fixed co-spherical segments, a helium balloon carries a gondola containing the focal optics and detector. We describe in more detail the Carlina concept, including versions equipped with an equatorial drive and a coudé train. The optical design with a clam-shell corrector of spherical aberration is optimized with a ray-tracing code. A two-element prototype of a sparse aperture, multi-element, optical dish has been built using a steerable balloon-suspended secondary optical structure. Following imaging and tracking tests with a single mirror, which give encouraging results, fringes have been obtained on Vega with a pair of closely spaced mirrors. We developed adjustment techniques for co-spherizing the mirrors within one or a few microns, using a light source at the curvature center. The absence of delay lines is a major simplification with respect to conventional interferometers, paving the way towards using hundreds or thousands of sub-apertures for producing direct images with rich information content. These results demonstrate the short-term feasibility of large Carlina hypertelescopes, with effective aperture size possibly reaching 1500 m at suitable terrestrial sites. Such interferometers will provide snapshot images of star surfaces, and of exo-planets if equipped with an adaptive coronagraph. Collecting areas comparable to those of ELTs appear feasible at a lower cost, while providing a higher resolution and similar limiting magnitude.

Key words. instrumentation: interferometers – instrumentation: high angular resolution – techniques: interferometric – instrumentation: adaptive optics – balloons

1. Introduction

Multi-element apertures with outer diameters larger than 200 m are required to obtain a usable number of resels in snapshot images of stellar surfaces, for a significant sample of the closest stars. A similar size begins to resolve the diameter of large Jupiter-like planets at 4 pc. But the 8-m size limitation generally quoted for monolithic mirrors, and the 100 m limitation foreseen for the mosaïc mirrors of the "Extremely Large Telescopes" currently studied, restrict their use for such science goals. The conventional interferometers using several telescopes have no such size limitation, and can therefore reach adequate resolution, but have a small number of apertures, limiting their ability to provide snap-shot images. Their cost and complexity are significantly increased by the delay lines (Mourard et al. 2003) which they incorporate, and the numerous reflections along the coudé trains degrade the luminosity.

In this article, we discuss various aspects of the hypertelescope architecture called Carlina (Labeyrie et al. 2002), which uses no delay-lines. Our group built in one and a half years a prototype Carlina at the Observatoire de Haute Provence (OHP). This prototype, currently equipped with only two of its mirror elements, uses balloon-suspended focal optics with equatorial tracking. As explained elsewhere (Labeyrie 1996; Pedretti et al. 2000; Gillet et al. 2003) hypertelescopes provide snapshot images, using a densified pupil. The densified-pupil intensifies the image obtained from a diluted aperture. At the combined Fizeau focus of a periodic dilute mirror, the image has a white central peak surrounded by many secondary dispersed peaks. Such Fizeau architectures become inefficient for large interferometers where the spacing of the sub-apertures

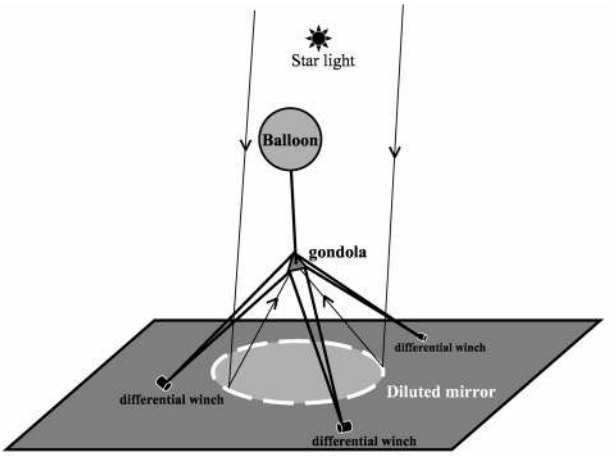

Fig. 1. A Carlina version using six computer-controlled winches to define the position and attitude of the focal beam combiner. These can be combined as three differential winches.

is typically much larger than their size. By densifying the exit pupil, the diffractive envelope of the combined image is shrunk and intensified while the secondary peaks are attenuated. Within a narrow field, the imaging properties of such instruments resemble those of ordinary telescopes.

In Sect. 2 we describe several architectures for a Carlina interferometer. In particular, we discuss ray-tracing results for a coudé version which relays a fixed image at ground level. We also discuss the optical design of a clam-shell corrector of spherical aberration used near the focal sphere of the Carlina. In Sect. 3 we describe the Carlina prototype which we built at Observatoire de Haute-Provence (OHP). We present initial results of star tracking in the presence of wind-induced oscillations at the balloon-borne camera. We conclude in Sect. 4 that Carlina hypertelescopes larger than 20 m are feasible in the near future.

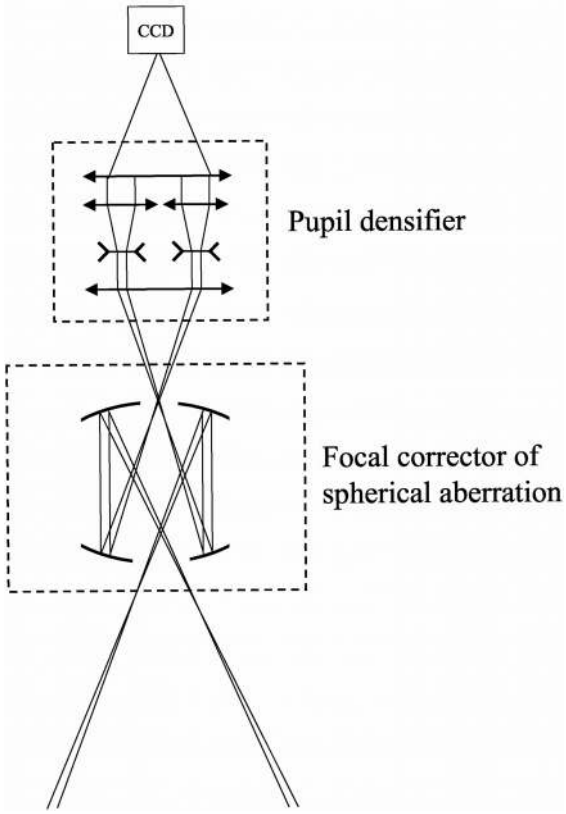

Fig. 2. The optics in the gondola will consist of a clam-shell corrector of spherical aberration, a pupil densifier and an EM-CCD camera. Adaptive optics will also be needed to correct the positioning errors of the fixed primary mirrors, in tip-tilt and piston, as well as the atmospheric seeing.

2. Architecture of a Carlina hypertelescope

Among the various possible hypertelescope architectures, the Carlina is analogous to the Arecibo radio telescope, although it uses a diluted primary mirror (Labeyrie et al. 2002). The primary mirror consists of many small mirrors, widely spaced with respect to their size. They have a shallow spherical curvature and are carried co-spherically by fixed supports inside a naturally concave site, canyon or crater (see Fig. 1). With stable bedrock and stiff, low-expansion mirror supports anchored in it, the initial adjustment of the dilute optical surface can survive, within tens of microns, during long periods, months or years. Passive supports then suffice for the mirror elements if adaptive corrections are implemented in the focal optics. The following description is based on this philosophy, although motorized mirror supports can be utilized at a later stage if needed.

Above this diluted primary mirror, a gondola is suspended from a helium balloon and constrained by cables to move along the half-radius focal sphere. The gondola contains focal optics equipped with a clam-shell corrector of spherical aberration, a pupil densifier and a detector (see Fig. 2). Three pairs of cables tie the gondola to computerized winches at ground level. The balloon keeps the cable tripod tensioned, thus ensuring its rigidity within the limits defined by cable sag, in response to gravity and wind-induced aerodynamic forces. The lengths of the six cables are determined by the three differential winches, thus defining the position and attitude of the gondola (see Fig. 1). The balloon typically oscillates in the wind while the tripod cables and the gondola remain little affected. The gondola's residual oscillations on the camera image globally moves the image without changing its shape. Unlike the jitter of component telescopes in conventional multi-telescope interferometers, which affects the relative positions and phases of component images in the beam combiner, the gondola's horizontal motion here produces a pure translation of the image. The vertical jitter produces pure defocus, and both can be corrected on-board with a simple x, y, z carriage and servo loop.

Unlike the case of a paraboloidal primary mirror, the spherical mirror allows continuous tracking, within its broad field, over hours by moving the gondola along the focal sphere. Unlike conventional interferometers no delay-lines are needed to maintain the optical path lengths when the instrument follows the star's diurnal motion. The segments of the spherical primary mirror are carried by separate rigid tripods.

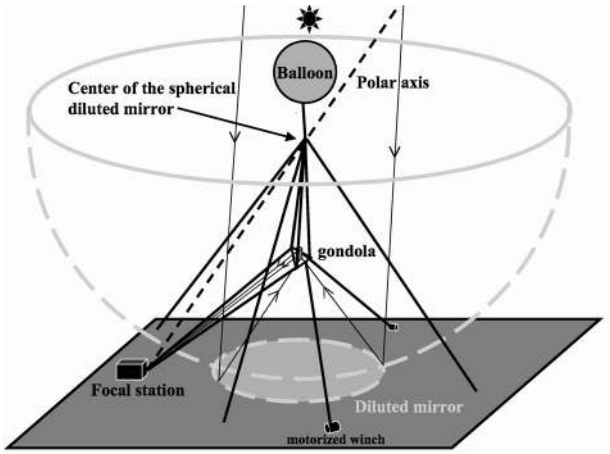

Fig. 3. Equatorial mode of star tracking with a Carlina. A single computer-controlled winch suffices to track the star.

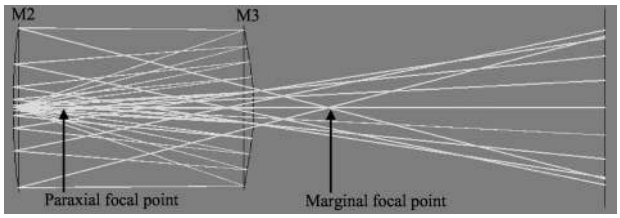

Fig. 4. Clam-shell corrector of spherical aberration and coma calculated with the Lasso code for F/2 acceptance. The paraxial and marginal foci of the primary mirror M1 (located far at right and not shown) are indicated. The corrected focus is at left, near the central hole of M2.

2.1. An equatorial version of Carlina

There are several ways of driving the gondola to track a star in the sky. In addition to the tri-axial scheme depicted in Fig. 1, which requires six computer-controlled winches, the cable arrangement which drives the gondola can be configured for equatorial tracking as sketched in Fig. 3. In this case, a single computer-driven winch suffices to track the diurnal motion. This cable arrangement can also carry a diode laser and metrology camera at the curvature center as described in Sect. 2.4, for monitoring the co-sphericity of the primary elements. The balloon must however be flown higher than in the tri-axial mode (Fig. 1).

In the equatorial tracking mode, the balloon is still tensioning a tripod of cables, but it is a fixed tripod of three cables rather than six, having its peak at the center of the primary mirror sphere (see Fig. 3). The gondola is suspended from the peak by three additional cables, at half the distance to the ground mirrors, which is the radius of the primary mirror. The gondola is thus constrained to move along the focal sphere. A pair of additional cables connects the gondola to the intersection of the ground plane with the polar axis containing the mirror's curvature center. This constrains the gondola to rotate about this polar axis. The rotation is driven by one more cable connecting the gondola to a motorized winch at ground level, which is opposed by a passive tensioning cable (see Fig. 3). With this architecture, the single computer-driven winch rotates the gondola about the polar axis, along the focal sphere, so as to track the star image with the gondola-borne camera. The length of the two cables from the gondola to the polar axis must be adjusted as a function of the star's declination.

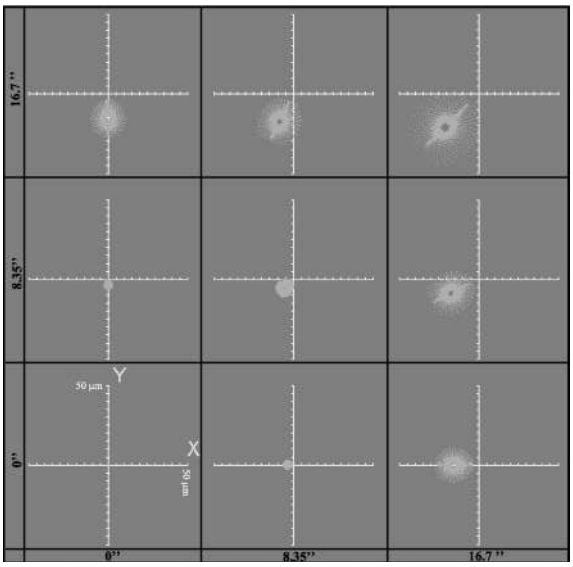

Fig. 5. Spot in the image plane of the clam-shell Mertz corrector for stars located up to 16.7″ (top-right) from the optical axis, as calculated with the Lasso code. The smaller scale units on the X and Y axes correspond to 5 microns.

2.2. The clam-shell corrector of spherical aberration

Spherical mirrors produce spherical aberration. We correct the spherical aberration of the equivalent large primary mirror with a clam-shell corrector (see Figs. 2, 6 and 7) described by Mertz (1996), which is located in the gondola close to the primary focal plane. This class of correctors, designed to meet Abbe's sine condition, corrects coma in addition to spherical aberration. The highly aspheric figures of the two mirrors are now within the fabrication capabilities of diamond-turning machines.

The equations for the corrector, found with the "RPLAN" code of Mertz are used as input for the Lasso ray-tracing code, developed by P. Rabou who further modified it for efficient interfacing with the Mertz routine. We also tried to use the Zemax code, but were unable to reach a comparable accuracy, owing to the limited order of the polynomial descriptions for the highly aspheric mirror surfaces. Tolerances on gondola oscillations were also assessed by analysing the off-axis image degradation with Lasso.

A given size of the effective aperture, utilizing a given number of mirror segments, requires a curvature radius which decreases if the acceptance angle or focal ratio of the Mertz corrector increases. For a given maximal zenith distance of sky coverage, the total number of mirror segments needed therefore decreases when the acceptance angle of the clam-shell corrector increases. A larger angle is therefore better, but the size of clam-shell correctors increases as the third power of the focal ratio. As a reasonable compromise we have chosen F/2 as the focal ratio, a value for which the corrector diameter can be less than 1% of the effective beam diameter at the primary mirror.

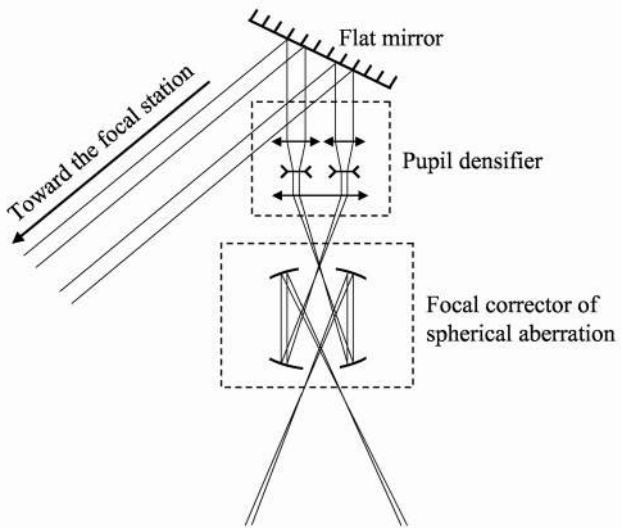

Fig. 6. Coudé feed in the gondola's focal optics. After the focal corrector of spherical aberration and the pupil densifier, using a pair of lens arrays, a flat mirror directs a coudé beam towards the focal station at ground level. The mirror must be rotated to accomodate different stellar declinations

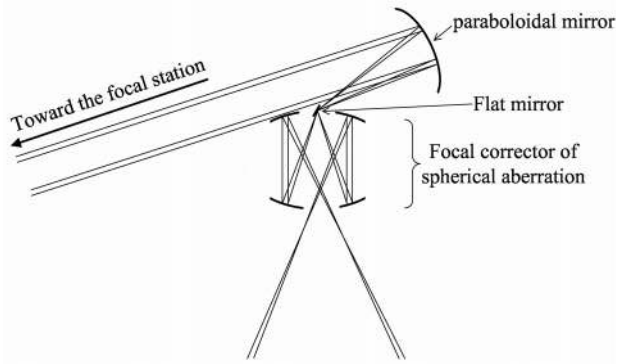

Fig. 7. Alternate scheme to Fig. 6 for coudé optics, using a small tiltable flat mirror and a paraboloidal mirror. The pupil densifier and the CCD are in the coudé station at ground level.

For the Carlina prototype described in Sect. 3, having a dilute spherical M1 mirror with 35.6 m focal length and F/2 focal ratio, we designed a Mertz corrector having two highly aspheric mirrors M2 and M3, about 160 mm in diameter. The spacing of M2 and M3 is 240 mm (Fig. 4). The size of the seeing-limited field is apparent in the spot diagrams of Fig. 5. A star at 16.7″ from the axis produces ∼1″ astigmatism in the image obtained with the 17.8 m primary spherical mirror (see Fig. 5). This field angle, corresponding to ±3 mm on the camera, specifies a similar stability tolerance for the gondola when high-resolution observations are made in the speckle interferometry mode, without adaptive optics nor even a servo guiding loop. Such image jitter on the camera is acceptable if the exposures are sufficiently short to freeze the drifting fringes.

The diffraction-limited half-field of the hypertelescope, with the 17.8 m aperture used around 600 nm wavelength, is similarly found to span about 3 arcsec. Like in the rather similar optical design of OWL it can be increased by correcting the residual astigmatism with two small additional mirrors after M3.

2.3. Coudé train feeding a ground station

It is possible to reflect the star light from the gondola towards a fixed coudé focus in a focal station at ground level (see Fig. 3). This is of interest for using bulky focal instruments, such as a spectrometer and adaptive optics, which do not fit easily in a small gondola and would require a larger balloon.

The coudé feed optics is located in the gondola after the focal corrector of spherical aberration and preferably also after the pupil densifier, typically containing a pair of lens arrays (Fig. 6). Another solution involves a small flat mirror in the corrected focal plane, angularly driven to accommodate changes in stellar declination, and an off-axis paraboloidal mirror which refocuses the light to the ground (see Fig. 7). The pupil densifier is here located in the focal station, but this requires in the gondola a wider pupil and paraboloidal mirror if the image's angular size is kept identical.

With the equatorial tracking scheme, the focal station is preferably aligned with the celestial pole and the curvature center of M1 (see Fig. 3) so as to receive a fixed image, only affected by field rotation and pupil drift, both correctible with a local rotating drive. In particular, the coudé beam can be collected by a classical telescope, which tracks the moving gondola. This telescope can be somewhat larger than strictly needed, to allow some tolerance of gondola tracking errors. The image can be stabilized with a tip-tilt corrector in the telescope.

For the latter coudé mode, we assessed with Zemax ray-tracing the combined effect of gondola oscillations and field aberrations in this stabilisation procedure, in the context of the preliminary testing of our prototype described in Sect. 3. At this stage there is a single 25 cm diameter primary mirror, of focal length 35.6 m, and it is not yet equipped with the spherical aberration corrector. The ray-tracing results are shown in Fig. 8.

A flat mirror and a paraboloidal mirror are located in the gondola (as in Fig. 7 but here without a clam-shell corrector) to re-focus star light on the large ground mirror of a 1.5 m telescope serving as a coudé collector in the focal station. Its large mirror, serving as a field mirror, forms a gondola image above its focal plane, where a lens, too small to appear on the drawing (see picture at the bottom-left of Fig. 8), relays the star image on a CCD. The spot diagram (bottom-right of Fig. 8) is obtained for a 5 mm gondola guiding error and $H = 4.5$ degrees hour angle. At transit, the star is on the axis of the single 25 cm primary mirror. The image is slightly degraded, mainly due to astigmatism, in the absence of a spherical aberration corrector for this preliminary configuration. The contribution of the gondola displacement is weak and the diffraction pattern is only slightly degraded. In this simulation we have optimized the focal length of the paraboloidal coudé mirror (mirror in Fig. 7 and in top-right of Fig. 8). If this focal length is large, the spot moves little on the ground telescope, in response to gondola oscilations but the coudé mirror has to be large and heavy to

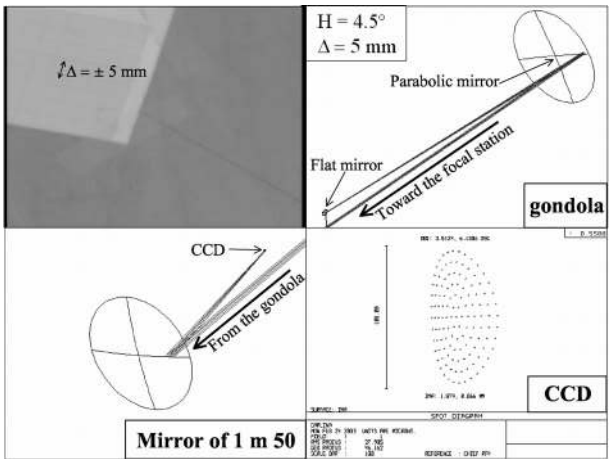

Fig. 8. The top-left of the figure shows a preliminary measurement of the residual oscillations at OHP. A gondola without optics is placed under a balloon at 35.6 m above ground. It oscillates by a few millimeters (rms) in the wind (Δ is the translation amplitude measured with a small telescope at ground level pointed at a sheet of millimetric paper glued on the gondola). The graph drawing at top-right and bottom-left shows a simple coudé train design, obtained with Zemax software. The corresponding spot diagram is at bottom right. At the top-right the gondola carries a small flat and a paraboloidal mirror (such as in Fig. 7 but without spherical aberration corrector). It is moved by 5 mm from the perfect position. At the bottom-left the light arrives on a focal station telescope focalized from the gondola. The light is translated by about one meter from the center of the mirror. The bottom-right picture shows the image on the CCD (scale: 100 μm). The CCD is placed behind a lens that is in a pupil plane.

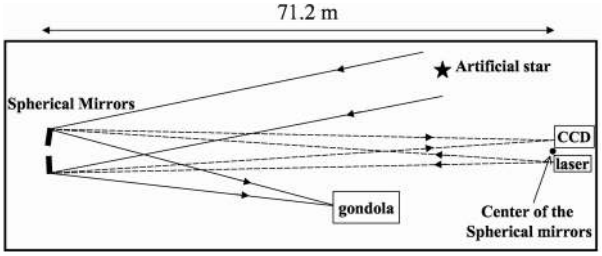

Fig. 9. Test optics arranged in the optical tunnel to develop phasing techniques. Two Carlina mirror segments spaced 35 cm apart produce fringes in the image of a point source located at their common center of curvature, 71.2 m away. A camera records the fringes, found by using a laser with adjustable coherence length. With a white source, the piston balance can be adjusted within one micron.

cover the full primary pupil. A 20 cm paraboloidal mirror with a focal length of 1 m is a good compromise for our prototype.

2.4. Coherencing and phasing the Carlina mirrors

In addition to the usual methods of acquiring stellar fringes with interferometers, a more direct procedure is usable in the case of Carlina architectures. It involves a light source at the curvature center (top of the tripod in Fig. 3) and a camera to observe the fringed return image produced by the primary mirror segments.

The light source is initially a laser diode having a coherence length comparable to the piston errors. It is then replaced by a white source to increase the piston sensitivity down to the seeing-limited value, below one micron.

The laboratory experiment sketched in Fig. 9 has shown that the method conveniently achieves the alignment of primary segments to a spherical surface without a stellar input. In comparison with existing interferometers, this internal metrology procedure for Carlina architectures is a significant simplification.

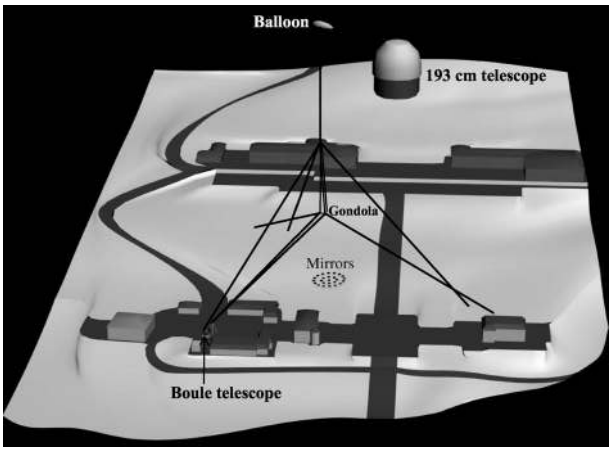

Fig. 10. Scale drawing of the Carlina prototype at the observatory. Pending crater sites, the flat ground is usable with a limited sky coverage in declination. The 4 mm Kevlar cables are thickened to make them visible. The 20-m dome of the 193 cm telescope appears on top to indicate the scale. The 1.5 m boule telescope at bottom-left, initially built as a prototype for the Optical Very Large Array (Arnold et al. 1999), is here potentially usable as a coudé collector receiving light from the focal gondola (described in Sect. 2.3).

3. Description of a Carlina prototype built at OHP and first results

At OHP we built a Carlina prototype system (Fig. 10), which is on flat ground, rather than in a crater, and therefore has a more limited celestial coverage. We have used the equatorial configuration described in Sect. 2.1 but not yet the coudé option, the gondola being equipped with a camera. The winches and other elements were positioned with a theodolite and a ranging laser, for a correct alignment of the virtual polar axis. The cables defining the fixed higher tripod have a 45 degree slope. In the rotating suspension the two cables which drive the gondola have a 22 degree slope. The gondola's stability is critically sensitive to the balance of cable tensions. We have developed a code and positioned the winches in order to optimize this balance.

The curvature radius of the dilute primary mirror is 71.2 m, thus requiring a gondola altitude of 35.6 m above the mirror elements. To minimize the celestial obscuration, the balloon is flown 140 m above ground level. At F/2 the sag of a 17.8 m spherical mirror is 0.56 m, requiring, if the ground is flat, supports with a similar height to carry the mirror segments located at the edge.

We designed and built a balloon shaped like a water drop, 12 m long, 4 m wide and with 80 kg carrying capacity.

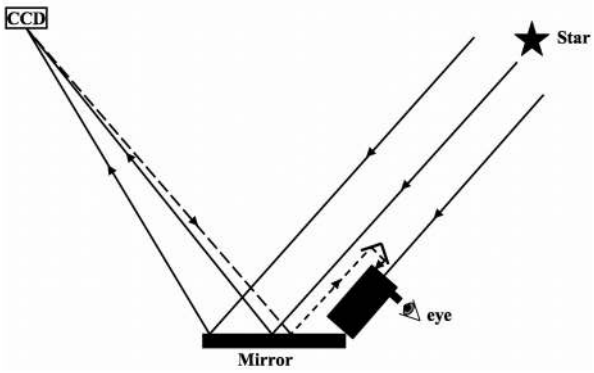

Fig. 11. Star acquisition system for Carlina. A small telescope is placed at the edge of the primary mirror segment and tracks the star. The light of a LED near the CCD in the gondola is reflected from the primary mirror segment towards a corner-cube reflector attached on top of the small telescope. The LED and the star are seen in the telescope eye-piece and must be superposed by moving the gondola.

Figure 10 shows the architecture of Carlina with several mirrors at ground level. To verify the star tracking performance and the level of wind-induced oscillations, we began with a single 25 cm diameter element of the primary mirror, supported by a 1×1 m concrete pier anchored to bedrock. Two more mirror segments were then installed on a second pier, located 9 m to the North. Each mirror cell is carried by three manual micrometer screws on top of a carbon fiber frame. For identical curvatures within $\lambda/8$, the Zerodur mirrors were controlled with respect to a convex full-size reference mirror.

The initial observations did not yet involve a clam-shell corrector since calculations had shown that the ensuing astigmatism is tolerable at moderate zenith distances (see Fig. 8).

3.1. Star acquisition system

A small guiding telescope is placed at the edge of the primary mirror segment and tracks the star. It carries a corner-cube reflector covering part of its aperture (see Fig. 11) to capture light from a LED source located near the CCD. This light is reflected from the primary mirror segment towards the star and part of it is retro-reflected into the guiding telescope (see Fig. 11). The LED and the star appear in the telescope eye-piece and must be superposed by moving the gondola. This superposition ensures the correct centering of the star image on the CCD. The field of the guiding telescope is preferably large to help pointing the star.

3.2. First light with a single primary mirror

The first light was obtained in March 2004 from the star "Psi Ursae Majoris" with a single mirror element. The gondola carried an electron-multiplier CCD of size 11.52×8.64 mm (E2V type L3C65-06P). We tracked the star for 30 min, before and after transit and the image remained most of the time on the CCD (see Fig. 12). The response to manual guiding corrections, made with a guiding paddle acting on the right-ascension and declination winches, proved faster than one second, in spite

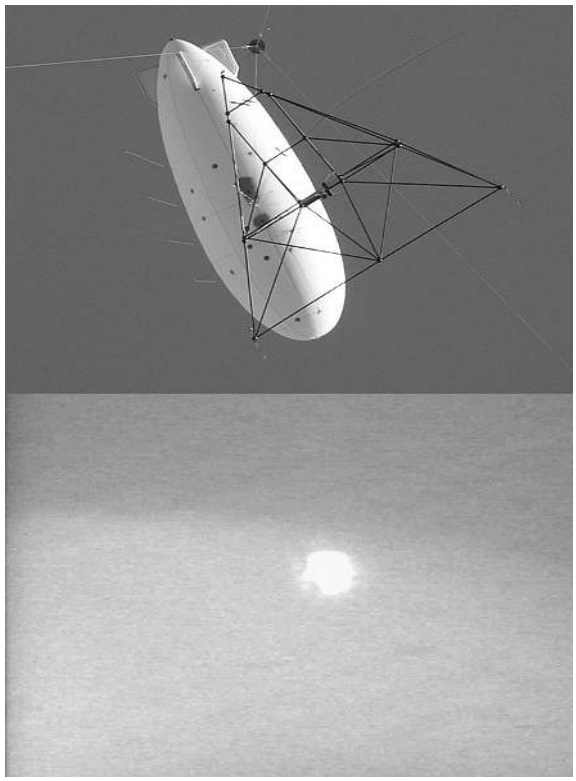

Fig. 12. *top*: tethered balloon, 140 m above ground. The black disc seen near the tail of the balloon is at the curvature center of the primary mirror, 71.2 m above it, and also at the top of the fixed cable tripod (see Fig. 3). The black triangle frame is the gondola, about 3 m in size and made of 16 mm diameter carbon fiber tubes, which carries the CCD, 35.6 m below this point. *Bottom*: first light for the Carlina prototype with a single primary mirror segment on star "Psi Ursae Majoris" obtained on 02/03/2004. The lateral field of the CCD image shown is about one arc minute and the size of the star image is close to 7 arcsec due to astigmatism, focus error and seeing.

of the Kevlar cable's intrinsic elasticity and that induced by sag. This encouraging result was obtained without any servo loop, after the observer had centered the star on the CCD with the pointing system described in Sect. 3.1. The tolerable wind velocity is estimated to be 5−10 km/h. With stronger winds, the balloon tends to orient itself across the wind, and a larger tail appears required to avoid this. However, the aerodynamics of the balloon can be improved for a better stability. For example, the commercially available Sky-Doc tethered balloons, equipped with a lift-generating sail, are quoted as standing wind velocities up to 148 km/h while maintaining a 58° slope on their tether.

3.3. First fringes

After the tracking tests, two additional mirror segments were installed on adjacent supports, about 9 m North of the first mirror. The coarse tip-tilt adjustment was made with retro-reflective sheeting at the curvature center. Two diode lasers were installed on the primary mirrors with their beams adjusted in the normal direction. The mirror attitude was then corrected with manual micrometer screws to superpose the laser spots

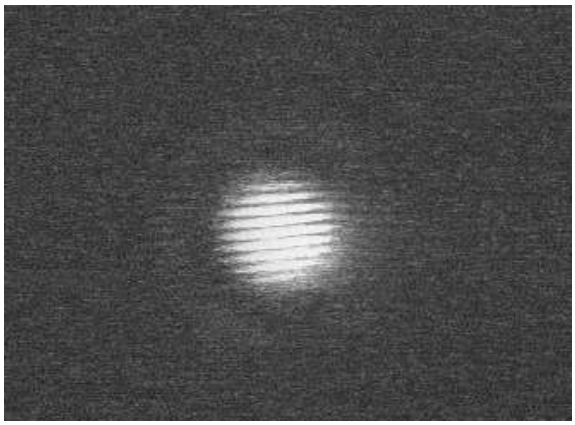

Fig. 13. Fringes obtained on Vega with the pair of adjacent mirrors stopped down to about 5 cm and providing a 40 cm baseline.

on the retro-reflective sheeting. The fine adjustment of tip-tilt and piston was made with a flat folding mirror, 25 cm in size and covering parts of both mirror segments, to make the curvature center easily accessible at ground level. The two mirrors were then adjusted for co-sphericity by the optical method mentioned in Sect. 2.4. The piston adjustment thus made with sub-micronic accuracy was found invariant during several night (from night to night). With the pair of adjacent mirrors, stopped down to 5 cm and providing a 40 cm baseline, Fizeau fringes were then obtained on Vega through a red filter with 100 nm bandwidth (see Fig. 13).

In spite of the short coherence length, a few microns, they appeared immediately when pointed and remained visible for more than one hour. We are now preparing to install a clam-shell corrector in the focal optics and a pupil densifier to use more widely spaced mirrors, up to 17.8 m.

The fringes obtained with the 40 cm baseline where not blurred by the imperfect star tracking. But the 50 times larger baselines to be used in forthcoming observations will be more sensitive to tracking drift. During a short exposure, the amount of drift must be limited to a fraction of the fringe spacing, both being expressed as celestial angles. The optimal exposure time thus defined does not depend on the pupil densification nor the pixel sampling in the camera. Exposures lasting a millisecond or less, with an electronically-shuttered EM-CCD camera, may become necessary, pending adaptive optical corrections of tracking errors and the higher-order wavefront errors caused by "seeing". Error signals usable for tracking corrections are: 1- the position of the star image on the camera, with its fringes; 2- images of a light pattern projected from ground, for example a "honeycomb" interference pattern from three coherent laser sources at ground level; 3- a sensitive accelerometer in the gondola. The actuators can be voice coils displacing a small lens or directly the CCD chip to minimize the reaction on the gondola structure and cables.

4. Conclusion and future work

In this article we have described several versions of the Carlina architecture for hypertelescopes. We have calculated optical designs having enough field of view to tolerate the oscillations of the gondola, up to a few millimetres. Their effect can be corrected with a servo guiding loop, acting as the first-order element of the adaptive optics which will be needed to correct the fixed piston errors arising from the imperfect positioning of the primary mirror segments, and the fluctuating piston errors generated by the atmosphere. Pending such adaptive corrections, the instrument is usable with full resolution in a speckle interferometry mode.

We describe the initial steps of constructing a prototype version at OHP. We have tracked the star "Psi Ursae Majoris", with a single primary mirror element attached to the bed rock, and a CCD in the focal gondola 35.6 m above. With two additional mirror segments, interference fringes were then obtained on Vega. Fringe acquisition proved much easier than with conventional interferometers, even in the presence of gondola oscillations with 1 mm amplitude and a period of a few seconds. Mirrors can indeed be cophased with the direct metrology method described in Sect. 2.4. To accomodate many mirrors providing larger baselines, approaching 20 m in this prototype Carlina, steps are now taken to up-grade the focal optics with a clam-shell corrector of spherical aberration and a pupil densifier system (Labeyrie 1996). Science observations are expected to begin in the speckle interferometry mode before installing servo guiding and adaptive optics. On Betelgeuse and Miras, the 18 m effective aperture size already achievable with our prototype allows 10×10 ressel snapshot images to be obtained with adaptive optics.

The design can in principle be extrapolated to large optical arrays with effective apertures spanning perhaps up to 1500 m and incorporating hundreds or thousands of mirror segments, at sites such as the "Caldera de Taburiente" crater in the Canarian islands (Labeyrie 2003).

Given the encouraging initial results obtained with our prototype we consider for the shorter term an intermediate step at the scale of a 50 to 200 m effective aperture size. Once equipped with adaptive optics (Martinache 2004; Borkowski et al. 2004) it will in principle provide snapshot images of star surfaces. The brighter exo-planets, such as 51 Peg b or Tau Bootes, become angularly separated from their parent star with apertures larger than 30 m at visible wavelengths. Their relative luminosity of 10^{-4} to 10^{-5} is within the detectability range if a coronagraph is added, possibly with post-focus adaptive cleaning.

It will be of interest to compare large Carlina arrays with ELTs in terms of science/cost efficiency. In the same way that large ELT designs evolved from the Keck I telescope, large hypertelescopes can be expected to evolve, on Earth and in space, from the prototype described here.

Acknowledgements. This research has been funded by Collège de France. This work evolved from a hypertelescope project, undertaken with O. Lardiere and S. Gillet (unpublished), specifically designed for observing Polaris. Some mechanical elements were fabricated by the technical group at OHP. The authors are grateful to P. Rabou from Grenoble Observatory, for his contribution to the optical ray-tracing with Lasso software. We are grateful to several students, F. Martinache, F. Ienna, A. Saglem and G. Le Marchand for their helpful contributions.

References

Andersen, T., Ardeberg, A., & Owner-Petersen, M. 2003, Euro 50 a 50 m adaptive optics telescope, Lund Observatory 2003, ed. T. Andersen, A. Ardeberg, & M. Owner-Petersen

Arnold, L., Lardière, O., & Dejonghe, J. 1999, Proceedings of the Bäckaskog Workshop on Extremely Large Telescopes, Backaskog Castle, Sweden, ed. T. Andersen, A. Ardeberg, & R. Gilmozzi, 132

Borkowski, V., Labeyrie, A., Martinache, F., & Peterson, D. 2004, A&A, submitted

Brunetto, E., Koch, F., & Quattri, M. 1999, Proceedings of the Bäckaskog Workshop on Extremely Large Telescopes, Backaskog Castle, Sweden, ed. T. Andersen, A. Ardeberg, & R. Gilmozzi, 109

Gillet, S., Riaud, P., Lardière, O., et al. 2003, A&A, 400, 393

Labeyrie, A. 1996, A&AS, 118, 517

Labeyrie, A. 2003, Proceedings SPIE 2nd Bäckaskog Workshop on Extremely Large Telescope, Bäckaskog Castle, Sweden, in press

Labeyrie, A. 2004, Removal of coronography residues with an adaptive hologram, for imaging exo-earths, EAS Publications Ser., ed. C. Aime, in press

Labeyrie, A., Le Coroller, H., Dejonghe, J., et al. 2002, Proceedings SPIE Hawaii, Hypertelescope imaging: from exo-planets to neutron stars, 4838

Martinache, 2004, J. Opt. A: Pure Appl. Opt., 6, 216

Mertz, L. 1996, Excursions in Astronomical Optics (New York: Springer-Verlag, Inc.)

Mourard, D., Abe, L., Domiciano, A., et al. 2003, Interferometry for Optical Astronomy II, ed. A. Wesley Traub, Proc. SPIE, 4838, 9

Pedretti, E., Labeyrie, A., Arnold, L., et al. 2000, A&AS, 147, 285